

Homotopy of periodic 2×2 matrices

Joseph E. Avron and Ari M. Turner

December 16, 2022

Abstract

We describe the homotopy classes of 2×2 periodic simple (=non-degenerate) matrices with various symmetries. This turns out to be an elementary exercise in the homotopy of closed curves in $\mathbb{R}^3/\{0\}$. The matrices represent gapped Bloch Hamiltonians in 1D with a two dimensional Hilbert space per unit cell.

1 Introduction

We study the homotopy classes of loops in the space of simple 2×2 matrices that satisfy various unitary or anti-unitary symmetries. This is motivated by the program of classifying the phases of insulating quantum matter [1, 2, 3, 4]. The classification is enriched by allowing for phases with symmetry [5, 6, 7].

An insulator is characterized by a (many body) ground state separated by a spectral gap which is bounded away from zero in the limit of large systems. The ground states of two insulators belong to the same phase if it is possible to interpolate between the two ground states without closing the gap. One can picture a phase diagram in a space of Hamiltonians with all possible parameters; the problem of finding phases can be described topologically as finding the connected components of the region corresponding to Hamiltonians with a gap¹. This is a challenging mathematical program, especially for interacting systems, as it concerns many-body quantum mechanics in the thermodynamic limit [10, 11, 12, 13, 14, 15, 16, 17].

The phases of topological insulators are of interest for the field of condensed matter because of their mobile edge states that are impervious to disorder[18, 19] and the search for quasi-particles with exotic statistics[9, 20, 21]. They are also of interest in quantum information theory because of their connections with computational complexity of many-body systems[22].

Arguably the simplest setting for studying phases of insulators is in the context of Bloch Hamiltonians² for non-interacting Fermions[1, 2]. Because

¹Further topological properties of this space are also interesting; for example, its fundamental group plays a role in quantized pumping:[8] and topologically protected quantum gates [9]

²For the study of models of free Fermions in disordered systems see e.g. [23, 24].

Bloch Hamiltonians have discrete translation symmetry, they can be studied directly in the limit of infinite systems. If the m lowest bands (for some m) are separated from the rest by a gap, an insulator with m Fermions per period can be formed by filling these states. We focus on the case where $m = 1$ (for spinless Fermions.)

A Bloch band can be represented by a loop $P(k)$ of orthogonal projections where k takes values in the Brillouin zone. The loop of band projection corresponds to a notion of a quantum state of a system with infinitely many particles.

Suppose that one restricts oneself to Bloch bands with a given symmetry, e.g. time-reversal. Two Bloch bands with projections $P_0(k)$ and $P_1(k)$ are said to be homotopic if there is a family of projections $P_t(k)$, jointly continuous³ in $(t \in [0, 1], k \in \text{BZ})$, respecting the symmetry, that interpolates between $P_0(k)$ and $P_1(k)$. This corresponds to the interpolations of the corresponding many-body quantum state of free Fermions. Describing the equivalence classes of Bloch bands with various symmetries is an interesting and non-trivial theoretical problem.

Our modest aim is to give an elementary invitation to this field by describing the homotopic classification of non-degenerate two-bands Bloch Hamiltonians in one dimensions with various symmetries, Table 1. This turns out to be a rather simple exercise in homotopy of curves in three dimension. This is a consequence of:

- The space of *simple* 2×2 Hermitian matrices is easy to characterize. It is essentially Euclidean 3 dimensional space with the origin removed: $\mathbb{R}^3/\{0\}$. In contrast, the space of $n \times n$ invertible Hermitian matrices, which describes insulators of more bands (see sec. 7) does not have such a simple characterization.
- One-dimensional Bloch Hamiltonians can be represented by closed curves in \mathbb{R}^3 hence questions regarding the homotopy of Bloch Hamiltonians reduce to questions about the homotopy of curves. The study of the homotopy classes of curves is the most intuitive parts of homotopy theory. This is in contrast with the study of the homotopy of Bloch Hamiltonians in higher dimensions which translates to the study of the homotopy of higher dimensional closed surfaces. This requires more advanced tools.

2 Bloch Hamiltonians with two bands

Consider a one-dimensional, single particle Hamiltonian acting on the Hilbert space

$$\ell^2(\mathbb{Z}) \otimes \mathbb{C}^2 \tag{2.1}$$

$j \in \mathbb{Z}$ labels the unit cell. Each unit cell hosts two degrees of freedom, e.g. a spin or a pair of atoms, labeled by $a \in \{0, 1\}$.

³The continuity follows from the continuity of the gapped Hamiltonian.

Symmetry	Constraint	$\{H(k), k \in \mathbb{S}\} \cong$
None	None	Z
TR_+	$H(k) = H^*(-k)$	Z
TR_-	$H(k) = YH^*(-k)Y$	\perp
PH_+	$H(k) = -ZH^*(-k)Z$	$\{\pm X, \pm R_1\}$
PH_-	$H(k) = -YH^*(-k)Y$	Z
BR	$H(k) = XH(-k)X$	$\{\pm X, \pm R_1\}$
SR	$H(k) = G_k H(-k) G_k^*$	$\pm Z$
$\bar{PH}_+ \circ \bar{TR}_+ = \text{Chiral}$	$\bar{H}(\bar{k}) = -\bar{Z}\bar{H}(\bar{k})\bar{Z}$	$\{\bar{R}_n n \in \mathbb{Z}\}$
$BR \circ TR_+$	$H(k) = XH^*(k)X$	$\{R_n n \in \mathbb{Z}\}$
$SR \circ TR_+$	$H(k) = G_k H^*(k) G_k^*$	$\pm Z$
$SR \wedge TR_+$	$H(k) = G_k H(-k) G_k^* = H^*(-k)$	$\pm Z$
$BR \wedge TR_+$	$H(k) = XH(-k)X = H^*(-k)$	$\{\pm R_n n \in \mathbb{Z}\}$
$\bar{PH}_+ \wedge \bar{TR}_+$	$\bar{H}(\bar{k}) = -\bar{Z}\bar{H}^*(-\bar{k})\bar{Z} = H^*(-\bar{k})$	$\{\pm R_n n \in \mathbb{Z}\}$
$PH_- \wedge TR_+$	$H(k) = -YH^*(-k)Y = H^*(-k)$	Y

Table 1: In the first column TR_{\pm} stands for time-reversal with $(TR_{\pm})^2 = \pm 1$, similarly for particle-hole symmetry PH_{\pm} . BR stands for bond-reflection and SR for site reflection. \wedge means that both symmetries are present and \circ that only the product is a symmetry. In the second column, X, Y and Z denote the Pauli matrices, and $G_k = \begin{pmatrix} e^{ik} & 0 \\ 0 & 1 \end{pmatrix}$. $*$ is complex conjugation. The third column gives the equivalence classes where $R_n = \begin{pmatrix} 0 & e^{-ink} \\ e^{ink} & 0 \end{pmatrix}$. The choice of matrices that represent the equivalence classes is not canonical. For example, in the first row, any 2×2 simple (=non-degenerate) periodic matrix is homotopic to any other non-degenerate matrix and the choice Z is just that, a choice. The entries above the top dashed line correspond to generating symmetries. The entries below show few composite symmetries. The list of composites is incomplete: Only products with TR_+ are listed.



Figure 1: A periodic array with two atoms per unit cell. The red ellipse shows the unit cell.

A one-particle lattice Hamiltonian is a self-adjoint infinite dimensional matrix with elements

$$\langle j, b | H | i, a \rangle = \langle i, a | H | j, b \rangle^* \quad (2.2)$$

A Bloch Hamiltonian is, by definition, translation invariant, i.e.

$$\langle j, b | H | i, a \rangle = \langle 0, b | H | i - j, a \rangle. \quad (2.3)$$

Translation invariance implies that H can be partially diagonalized by Fourier transform (going to momentum space). For the Fourier transform to be well defined one needs to assume locality, i.e.

$$\sum_j \left| \langle 0, b | H | j, a \rangle \right| < \infty \quad (2.4)$$

Locality, Eq. 2.4, implies that the Bloch Hamiltonian $H(k)$ defined by

$$H_{ba}(k) = \sum_j \langle j, b | H | 0, a \rangle e^{-ikj} \quad (2.5)$$

is a continuous periodic matrix-valued function of k . $H(k)$ is Hermitian for each k since

$$\begin{aligned} H_{ba}(k) &= \sum_j \langle j, b | H | 0, a \rangle e^{-ikj} \\ &= \sum_j \langle 0, a | H | j, b \rangle^* e^{-ikj} \\ &= \left(\sum_j \langle -j, a | H | 0, b \rangle e^{-ikj} \right)^* \\ &= H_{ab}^*(k) \end{aligned} \quad (2.6)$$

$H(k)$ is not uniquely defined: There is a k -dependent gauge freedom associated with the choice of unit cell, which we shall return to in section 3.1.

Without loss of generality⁴, we may replace $H(k)$ by its traceless part

$$H(k) \mapsto H(k) - \mathbb{1} \operatorname{Tr} H(k)/2 = \begin{pmatrix} z_k & x_k - iy_k \\ x_k + iy_k & -z_k \end{pmatrix}, \quad (2.7)$$

The spectrum of $H(k)$ has two (continuous) bands with opposite energies, see Fig. 2

$$E^2(k) = -\det H(k) = \mathbf{x}_k \cdot \mathbf{x}_k, \quad \mathbf{x}_k = (x_k, y_k, z_k) \quad (2.8)$$

⁴This amounts to a time-dependent gauge transformation.

Since the spectrum of the Bloch Hamiltonian is the same as the union of the spectrum of $H(k)$ over k , insulators with a gap are characterized by the gap condition

$$E^2(k) > 0 \quad \forall k \in [-\pi, \pi] \quad (2.9)$$

3 Periodic matrices and loops in \mathbb{R}^3

A traceless, Hermitian 2 matrix can be represented geometrically by a point in \mathbb{R}^3

$$H(\mathbf{x}) = xX + yY + zZ, \quad \mathbf{x} = (x, y, z) \in \mathbb{R}^3 \quad (3.1)$$

X, Y, Z are the three Pauli matrices. Periodic, traceless, Hermitian matrices can be represented as closed loops in \mathbb{R}^3 .

Taking the gap condition into account, $H(k)$ can be represented by a closed continuous curve in Euclidean 3 space with the origin removed

$$\gamma = \{\mathbf{x}_k | -\pi \leq k \leq \pi\} \in \mathbb{R}^3 / \{0\}. \quad (3.2)$$

From this point of view we can see that Hamiltonians are connected to one another within the space of gapped Hamiltonians if they are represented by closed curves that are homotopic. (If two curves are homotopic, the curves connecting them can be approximated by trigonometric polynomials in k while still avoiding the origin—hence there are finite range Hamiltonians corresponding to them.)

The space of traceless Hermitian 2×2 matrices, being isomorphic to \mathbb{R}^3 has no interesting topology: it is contractible. The space of non-degenerate (aka simple) matrices is isomorphic to Euclidean 3 space with the origin removed and is homotopic to the 2-sphere:

$$\mathbb{R}^3 / \{0\} \simeq \mathbb{S}^2 \quad (3.3)$$

which has interesting topology⁵.

Now although this space is not contractible, it is simply connected, so all Hamiltonians are homotopic to one another. Hence the space of Hamiltonians with a gap consists of one phase). The phase diagram will be disconnected when symmetries are introduced however⁶.

3.1 Gauge ambiguity of Bloch Hamiltonians

Changing the unit cell permutes the basis vectors

$$U_\ell |j, b\rangle = |j + b\ell, b\rangle, \quad b \in \{0, 1\}, \quad \ell \in \mathbb{Z} \quad (3.4)$$

Fig. 2 is an example with $\ell = 1$. H transforms by

⁵The first few homotopy groups of the 2-sphere are

$$\pi_0(\mathbb{S}^2) = \pi_1(\mathbb{S}^2) = 0, \quad \pi_2(\mathbb{S}^2) = \pi_3(\mathbb{S}^2) = \mathbb{Z}, \quad \pi_4(\mathbb{S}^2) = \mathbb{Z}_2, \quad \dots$$

⁶In two and higher dimensions, there are distinct phases without introducing symmetries.

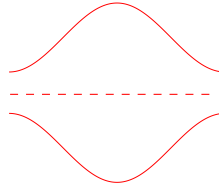


Figure 2: The spectrum of $H(k)$ has two, mirror images, bands, separated by a gap.

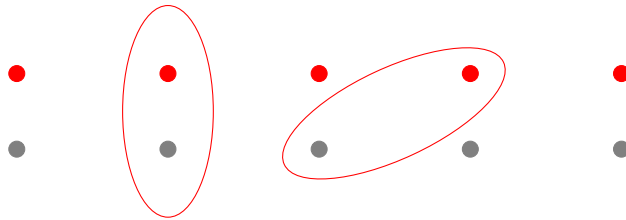


Figure 3: The two red ellipses correspond to two different choices of unit cell. Changing the unit cell is a gauge transformation (=diagonal unitary) acting on $H(k)$.

$$\langle j, b | U_\ell^\dagger H U_\ell | i, a \rangle = \langle j + b\ell, b | H | i + a\ell, a \rangle \quad (3.5)$$

and $H(k)$ by

$$(U_\ell^\dagger H(k) U_\ell)_{b,a} = H_{ba}(k) e^{ik\ell(b-a)} \quad (3.6)$$

The action of U_ℓ in k -space is implemented by a diagonal, k -dependent, unitary 2×2 matrix:

$$U_\ell = \begin{pmatrix} 1 & 0 \\ 0 & e^{-ik\ell} \end{pmatrix}, \quad \ell \in \mathbb{Z} \quad (3.7)$$

4 Symmetries

This section is a multi-lingual dictionary that translates several symmetries of H in coordinate space to symmetries of $H(k)$ and then to symmetries of the corresponding loops γ , allowing us to determine the homotopy classes for each type of symmetry in the next section. (One can alternate between the two sections in order to understand each symmetry all at once.) Chiral symmetry and its combinations with other symmetries are relegated to the appendix.

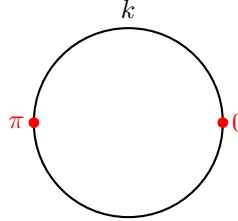


Figure 4: The one dimensional Brillouin zone is a circle parameterized by the angular variable k . The reflection $k \mapsto -k$ leaves the two points $k = 0$ and $k = \pi$ invariant.

4.1 Time reversal

Time-reversal Θ is an anti-unitary map in Fock space. This is a consequence of the presence of i in the Heisenberg equation

$$\dot{\mathbf{A}} = i[\mathbf{H}, \mathbf{A}] \quad (4.1)$$

where \mathbf{A}, \mathbf{H} are operators in Fock space. Since $\{\Theta, \frac{d}{dt}\} = 0$ it follows that $\{\Theta, i\} = 0$ and so is anti-linear.

Now for the problem studied in this article, it is useful to represent time-reversal as an operation on single-particle states. By definition, time reversal maps particle creation to particle creation⁷, although a creation operator for a given state may map to a creation operator for some other state:

$$\Theta(a^\dagger(f)) = a^\dagger(\Theta(f)). \quad (4.2)$$

The bold and ordinary Θ 's refer respectively to the transformation of the creation operator and the transformation of the wave function associated to it. As $a^\dagger(f)$ is linear in f and $a(g)$ is anti-linear in g , it follows from the commutation relation that $\Theta(f)$ is anti-unitary

$$\{\Theta(a(g)), \Theta(a^\dagger(f))\} = \{a(\Theta g), a^\dagger(\Theta f)\} = \Theta\langle g|f \rangle = \langle f|g \rangle \quad (4.3)$$

Hence

$$\Theta = U \circ * \quad (4.4)$$

with U unitary and $*$ complex conjugation.

One reasonably assumes that reversing time twice produces an un-observable effect, i.e., it is a pure phase. Then it follows that, since Θ commutes with Θ^2 , the only phase consistent with the anti-unitarity of Θ is ± 1 , i.e.:

$$\Theta^2 = UU^* = \pm \mathbb{1} \implies U = \pm U^t \quad (4.5)$$

Under unitary change of bases W

$$\Theta \mapsto W\Theta W^\dagger = WUW^t \circ * \quad (4.6)$$

⁷The operation that maps creation to annihilation is particle-hole transformation.

U then undergoes a congruence transformation.

We assume that U act on the internal coordinates $|a\rangle$ in real space while leaving the spatial coordinate j unchanged. Equivalently, in terms of the Bloch Hamiltonian,

$$\Theta H(k)\Theta^{-1} = U H^*(-k) U^\dagger \quad (4.7)$$

By definition, $H(k)$ is time-reversal invariant if

$$H(k) = U H^*(-k) U^\dagger \quad (4.8)$$

for an appropriate unitary $U = \pm U^t$.

4.1.1 Time reversal with $\Theta^2 = \mathbb{1}$

Any symmetric unitary 2×2 matrix U is congruent to the identity⁸. This follows from the fact that U can be written as

$$U(\theta, \phi, \alpha) = e^{i\alpha} [\mathbb{1} \cos \theta + i \sin \theta (X \cos \phi + Z \sin \phi)] \quad (4.9)$$

U has a symmetric square root $\sqrt{U} = U(\theta/2, \phi, \alpha/2)$. It follows that

$$U = \sqrt{U} \mathbb{1} (\sqrt{U})^t, \quad (4.10)$$

- Say $U = \mathbb{1}$: The loop $\gamma \in \mathbb{R}^3$ is symmetric under reflection in y

$$z_k = z_{-k}, \quad x_k = x_{-k}, \quad y_k = -y_{-k} \quad (4.11)$$

and is anchored at $k = 0, \pi$ to the punctured $x - z$ plane, see Fig. 5.

4.1.2 Time reversal with $\Theta^2 = -\mathbb{1}$:

There is a unique anti-symmetric matrix U up to multiplication by a scalar. Since an overall phase is for free in an anti-unitary transformation, we may chose $U = Y$

$$\Theta = Y \circ *, \quad Y = \begin{pmatrix} 0 & -i \\ i & 0 \end{pmatrix} \quad (4.12)$$

whose action on $H(k)$ is

$$\Theta H(k)\Theta^{-1} = Y H^*(-k) Y = -H(-k). \quad (4.13)$$

The last equality can be checked by using the representation Eq. 3.1 for $H(-k)$. A 2×2 matrix $H(k)$ is (Fermionic) time reversal symmetric if

$$H(k) = -H(-k) \quad (4.14)$$

- The loop γ is inversion symmetric

$$z_k = -z_{-k}, \quad x_k = -x_{-k}, \quad y_k = -y_{-k} \quad (4.15)$$

and is anchored at the origin at $k = 0$ and $k = \pi$

$$\mathbf{x}_0 = \mathbf{x}_\pi = 0 \quad (4.16)$$

This is Kramers's degeneracy. This family of matrices is not simple and shall not be considered further.

⁸We thank Oded Kenneth for the proof below.

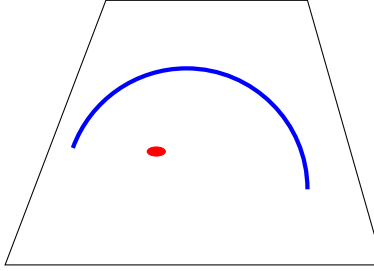


Figure 5: The curve γ_- associated with time-reversal symmetric Hamiltonians is anchored on the punctured $x - z$ plane. The rest of the loop is fixed by symmetry of reflection in the plane.

4.2 Particle-Hole transformation

Particle-hole transformation \mathbf{C} maps particle creation to particle annihilation:

$$\mathbf{C}(a^\dagger(f)) = a(C(f)) \quad (4.17)$$

The particle creation operator $a^\dagger(f)$ depends linearly on f while the annihilation operator is anti-linear. \mathbf{C} (the many-body operator) must commute with i in order to preserve the direction of time. Thus, in order for both sides to be linearly dependent on f , C (the one-particle operator) must be anti-linear. Being anti-unitary, C comes in two varieties

$$C^2 = \pm \mathbb{1} \quad (4.18)$$

just like time-reversal.

4.3 Particle-Hole symmetry

By definition, H is particle-hole symmetric if it anti-commutes with \mathbf{C}

$$\{\mathbf{C}, H\} = 0 \quad (4.19)$$

For Bloch Hamiltonians we get from Eq. 4.8

$$H(k) = -UH^*(-k)U^\dagger \quad (4.20)$$

We then have:

4.3.1 If $\mathbf{C}^2 = 1$:

Since all anti-unitary transformations are equivalent to $\mathbb{1} \circ *$, they are equivalent to one another. We pick $U = Z$.

- The loop $\gamma \in \mathbb{R}^3$ is symmetric under π rotation around the x -axis,

$$z_k = -z_{-k}, \quad x_k = x_{-k}, \quad y_k = -y_{-k} \quad (4.21)$$

and is anchored at $k = 0, \pi$ to the punctured x -axis, Fig. 12.

4.3.2 $C^2 = -1$:

As we have seen for time-reversal

$$C = Y \circ * \quad (4.22)$$

whose action on $H(k)$ is

$$CH(k)C^{-1} = YH^*(-k)Y. \quad (4.23)$$

So a 2×2 matrix $H(k)$ is particle-hole symmetric if

$$H(k) = -YH^*(-k)Y = H(-k) \quad (4.24)$$

- The loop γ is self-retracing

$$z_k = z_{-k}, \quad x_k = x_{-k}, \quad y_k = y_{-k} \quad (4.25)$$

and is not anchored at $k = 0$ and $k = \pi$.

4.4 Bond reflection symmetry

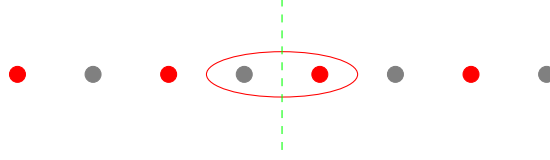


Figure 6: Bond reflection symmetry is a reflections about the green dashed line

Bond reflection (see Fig. 4.4) permutes the basis vectors

$$(R_b)(j, a) = (-j, a \oplus 1) \quad (4.26)$$

where \oplus is addition modulo 2. The transformation reflects unit cells, and exchanges the “atoms” in a unit cell.

The action of bond-reflection on the Hamiltonian in the coordinate basis is

$$R_b(h)_{j,b;i,a} = h_{-j,b \oplus 1; -i, a \oplus 1} \quad (4.27)$$

It follows from Eq. 2.5 that the action in k -space is

$$R_b(H)_{b,a}(k) = H_{b \oplus 1, a \oplus 1}(-k) \quad (4.28)$$

In matrix form:

$$R_b(H(k)) = \begin{pmatrix} -z_{-k} & x_{-k} + iy_{-k} \\ x_{-k} - iy_{-k} & z_{-k} \end{pmatrix} = XH(-k)X \quad (4.29)$$

R_b is an involution:

$$(R_b)^2 = \mathbb{1} \quad (4.30)$$

$H(k)$ is bond-reflection symmetric if

$$H(k) = XH(-k)X \quad (4.31)$$

- γ is symmetric under a rotation by π about the x-axis:

$$z_k = -z_{-k}, \quad x_k = x_{-k}, \quad y_k = -y_{-k} \quad (4.32)$$

and is anchored to the punctured x axis at 0 and π .

4.5 Site reflection symmetry

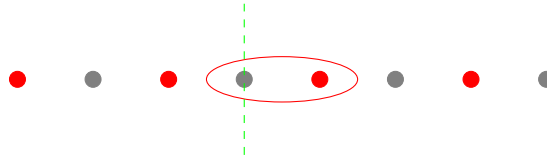


Figure 7: Site reflection symmetry is a reflection about the green dashed line

Reflection about a site (see Fig. 4.5) permutes the basis vectors by

$$(R_s)(j, a) = (-j - a, a) \quad (4.33)$$

The permutation mixes different unit cells. Its action on $h_{j,b;i,a}$ is given by

$$R_b(h)_{j,b;i,a} = h_{-j - b, b; -i - a, a} \quad (4.34)$$

By Eq. 2.5 site reflection acts in k -space by

$$R_s(H)_{b,a}(k) = H_{b,a}(-k) e^{ik(b-a)} \quad (4.35)$$

and in matrix form

$$R_s(H(k)) = G_k H(-k) G_k^\dagger, \quad G_k = \begin{pmatrix} 1 & 0 \\ 0 & e^{ik} \end{pmatrix} \quad (4.36)$$

$H(k)$ is site-reflection symmetric if

$$H(k) = G_k H(-k) G_k^\dagger \quad (4.37)$$

- γ_- and γ_+ are related by:

$$z_k = z_{-k}, \quad \begin{pmatrix} x_k \\ y_k \end{pmatrix} = \begin{pmatrix} \cos k & -\sin k \\ \sin k & \cos k \end{pmatrix} \begin{pmatrix} x_{-k} \\ y_{-k} \end{pmatrix} \quad (4.38)$$

- γ is anchored at one end on the punctured z -axis

$$x_{\pm\pi} = y_{\pm\pi} = 0, \quad |z_{\pm\pi}| > 0 \quad (4.39)$$

Example 4.1 A Bloch Hamiltonian with site reflection symmetry is

$$H(k) = \begin{pmatrix} v & 1 + e^{-ik} \\ 1 + e^{ik} & -v \end{pmatrix} \quad (4.40)$$

5 Homotopy of periodic 2×2 matrices

Two Bloch Hamiltonians are homotopic if one can be deformed to the other, within a given symmetry class, without closing the gap. In the case of 2×2 (periodic) matrices the question reduces to the homotopy of continuous closed loops $\gamma \in \mathbb{R}^3/\{0\}$ that are constrained by the symmetry. In principle, this constraint could have complicated the question of homotopy equivalence. Fortunately, for most of the constraints we consider, this is not the case.

When one of the symmetries exchanges k and $-k$, the problem can be simplified as follows. Write γ as a composition of two curves

$$\gamma = \gamma_- \circ \gamma_+ \quad (5.1)$$

where

$$\gamma_- = \{\mathbf{x}_k | -\pi \leq k \leq 0\}, \quad \gamma_+ = \{\mathbf{x}_k | 0 \leq k \leq \pi\} \quad (5.2)$$

The symmetry says that γ_- determines γ_+ (and vice versa), and imposes constraints on the end-points of γ_\pm . (In some cases γ is also constrained to be planar.) Then any homotopy of the full curve γ is determined by the homotopy of the arc γ_- , with the end-points required to satisfy the constraint. The homotopy equivalence of different curves γ_- is then an elementary exercise. Homotopy classifications for chiral symmetry are relegated to an appendix.

5.1 No symmetry

$\mathbb{R}^3/\{0\}$ is simply connected. This means that every (continuous) loop can be contracted to a point. Since $\mathbb{R}^3/\{0\}$ is connected, every point is homotopic to every other point. Hence any Bloch Hamiltonian is homotopic to any other Bloch Hamiltonian,

$$\{H(k), k \in \mathbb{S}\} \cong Z, \quad (5.3)$$

The k -independent Hamiltonian Z describes a disconnected chain of 2-level atoms, whose many-body ground state is a (formal) pure product state

$$\prod_j |1\rangle_j. \quad (5.4)$$

Pure product states are taken as the defining property of a trivial phase.

5.2 Time reversal $\Theta^2 = 1$

Here the closed loop γ is symmetric under reflection in y -axis, and is anchored to the $x - z$ plane for $k = 0, \pi$, see Eq. 4.11.

Since γ avoids the origin, it is homotopic to $\hat{\gamma}$ on the unit sphere

$$\hat{\gamma} = \{\hat{\mathbf{x}} | \mathbf{x} \in \gamma\}, \quad \hat{\mathbf{x}} = \frac{\mathbf{x}}{|\mathbf{x}|} \quad (5.5)$$

with end-points anchored to a punctured equatorial plane, see Fig. 5.

$\hat{\gamma}_-$ can be deformed provided it respects the anchoring to an equator. $\hat{\gamma}_+$ follows by the symmetry constraint. Suppose first that the anchoring points coincide. Since \mathbb{S}^2 is simply connected, $\hat{\gamma}_-$ can be contracted to a point. The mirror image $\hat{\gamma}_+$ will contract simultaneously.

In the case that the anchoring points do not coincide the end-point at $k = \pi$ can be brought to the end-point at $k = 0$ by applying a rotation around the y -axis $R_y(\phi)$ (since both lie on the unit circle in the $x - z$ plane). The angle ϕ is imagined to increase continuously from 0 until the points coincide. The k dependent rotation

$$R_y(k\phi/\pi)\hat{\mathbf{x}}_k, \quad 0 \leq k \leq \pi \quad (5.6)$$

is a homotopy of $\hat{\gamma}_-$ which respects the gap condition, since a rotation preserves the length of vectors. Hence $\hat{\gamma}_-$ is homotopic to a point. Finally, since the equator in the $x - z$ plane is connected, all points in it are homotopic.

It follows that the space of time reversal 1D Bloch Hamiltonians with a gap condition has a single component under homotopy:

$$\{H(k), k \in \mathbb{S}\} \cong \mathbb{Z} \quad (5.7)$$

5.3 Particle-Hole symmetry

5.3.1 $C^2 = 1$

The closed loop γ is symmetric under rotation by π about the x -axis, and is anchored to the (punctured) x -axis for $k = 0, \pi$, see Eq. 4.21. γ is homotopic to $\hat{\gamma}$ on the unit sphere, anchored at the poles:

$$\hat{\mathbf{x}}_0, \hat{\mathbf{x}}_\pi = \pm(1, 0, 0) \quad (5.8)$$

When the anchoring points coincide $\hat{\gamma}_-$ is homotopic to a point. In the case that the anchoring points are antipodal, $\hat{\gamma}_-$ can be continuously shortened to a geodesic. This means that $\hat{\gamma}$ is homotopic to a circle. In conclusion, a particle-

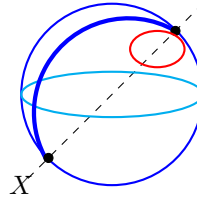


Figure 8: γ_- with particle-hole symmetry. The blue spherical curve is anchored at $x = \pm 1$. The red one is anchored at $x = -1$.

hole symmetric Hamiltonian is homotopic to an element of a set with four elements:

$$H(k) \cong \{\pm X, \pm R_1\} \quad (5.9)$$

($R_1 \cong R_{-1}$ by a π rotation about the x axis.) The four elements are distinguished by the combinations of signs of the anchoring points on x .

$\pm X$ is a Bloch Hamiltonian with disconnected cells, so the ground states are pure product states

$$\prod_j |+\rangle_j, \quad \prod_j |-\rangle_j, \quad |\pm\rangle = \frac{|0\rangle \pm |1\rangle}{\sqrt{2}} \quad (5.10)$$

representing trivial phases, (while the Hamiltonians $\pm R_1$ have edge states at the ends of the chain).

5.3.2 $C^2 = -1$

The loop γ is self-retracing and is not anchored. Since $\mathbb{R}^3/\{0\}$ is simply connected, the loop is null-homotopic and

$$\{H(k), k \in \$\} \cong Z \quad (5.11)$$

5.4 Bond reflection symmetry

The curve γ is anchored on the punctured x -axis. This is the same scenario as in the previous section and hence

$$\{H(k), k \in \$\} \cong \{\pm X, \pm R_1\} \quad (5.12)$$

The families $\pm X$ describe trivial phases where the full bands are pure product states

$$\prod_j |+\rangle_j, \quad \prod_j |-\rangle_j \quad (5.13)$$

5.4.1 Both bond reflection and time reversal symmetry

For $H(k)$ with bond reflection and (Bosonic) time reversal one has:

- γ lies in the $x - y$ plane
- γ is anchored on the punctured x -axis

Since the punctured plane is not simply connected, loops are distinguished not just by the anchoring points, but also by their winding, hence

$$\{H(k), k \in \$\} \cong \{\pm R_n | n \in \mathbb{Z}\} \quad (5.14)$$

5.4.2 Composition of Bond Reflection and Time Reversal

For Hamiltonians with only one symmetry, the *composition* of time reversal and bond reflection, the possible classes are

$$\{H(k), k \in \$\} \cong \{R_n | n \in \mathbb{Z}\}. \quad (5.15)$$

γ is restricted to the $x - y$ plane, and there is no additional symmetry between the two halves of γ . Thus the Hamiltonian's class is determined by the winding number around $(0, 0)$.

5.5 Site reflection symmetry

The loop γ of Eq. 4.38 is anchored at $k = \pm\pi$ to the punctured z-axis:

$$x_{\pm\pi} = y_{\pm\pi} = 0, \quad |z_{\pm\pi}| > 0 \quad (5.16)$$

γ_- can be contracted to the anchoring point at $k = -\pi$ and the contraction of γ_+ then follows by symmetry.

$$\mathbf{x}_k(t) = \mathbf{x}_{(1-t)k-t\pi}, \quad t \in [0, 1] \quad (5.17)$$

Since $\mathbf{x}_k \neq 0$ for all k , the map is a homotopy in $\mathbb{R}^3/\{0\}$. It follows that gapped, site symmetric Bloch Hamiltonians are homotopic to

$$\{H(k), k \in \mathbb{S}\} \cong \pm Z \quad (5.18)$$

The corresponding (many-body) ground state represents a trivial phase as it is (formally) a pure product state,

$$\prod_j |1\rangle, \quad \prod_j |0\rangle. \quad (5.19)$$

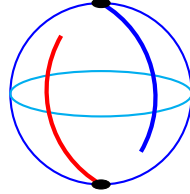


Figure 9: Curves anchored at the north pole are homotopic to the north pole. And curves anchored at the south pole are homotopic to the south pole. This shows that the space of loops is made of two disconnected sets.

5.5.1 Both site reflection and time reversal symmetry

So far, the classification has been equivalent either to homotopy classification of loops or arcs (with anchoring conditions) in some space. This is not anymore the case for Bloch Hamiltonians with time reversal and site reflection symmetry.

Time reversal forces $x_k = x_{-k}$ and $y_k = -y_{-k}$. Substitution in Eq. 4.38, the site-reflection condition, gives an equation that constrains the curve:

$$\begin{pmatrix} \cos k - 1 & \sin k \\ \sin k & -\cos k - 1 \end{pmatrix} \begin{pmatrix} x_k \\ y_k \end{pmatrix} = 0 \quad (5.20)$$

Since the determinant vanishes there is a solution, determined up to a factor

$$(x_k, y_k) = \lambda_k \left(\cos \frac{k}{2}, \sin \frac{k}{2} \right), \quad \lambda_{\pm\pi} = 0 \quad (5.21)$$

while z_k is arbitrary. γ_- is an arc that is anchored at $-\pi$ on the punctured z -axis, and the arc can be contracted to the north or to the south pole—provided it satisfies the constraint, for example,

$$z_k(t) = (1-t)z_k + tz_\pi, \quad (x_k, y_k) = (1-t)\lambda_k \left(\cos \frac{k}{2}, \sin \frac{k}{2} \right) \quad (5.22)$$

Hence there are two homotopy classes

$$\{H(k), k \in \$\} \cong \pm Z \quad (5.23)$$

5.5.2 Composition of Time Reversal and Site Reflection

The case $TR \circ SR$ is interesting as it leads to homotopy classification of a path that is not closed but has different constraints. The symmetry implies

$$(x_k, y_k) = \lambda_k \left(\cos \frac{k}{2}, \sin \frac{k}{2} \right) \quad (5.24)$$

This condition constrains (x_k, y_k, z_k) to lie in a plane that rotates about the z -axis as a function of k , the plane whose angle with the $x - z$ plane is $\frac{k}{2}$. If (x_k, y_k, z_k) is described using coordinates within the rotating plane, it will trace out a curve in two dimensions. However, the plane rotates 180° so the points at π and $-\pi$ should be mirror images of one another in the rotation axis. To see this clearly, use the coordinates λ_k, z_k , defined by

$$(x_k, y_k, z_k) = \lambda_k \left(\cos \frac{k}{2}, \sin \frac{k}{2}, 0 \right) + z_k(0, 0, 1). \quad (5.25)$$

Periodicity of γ implies $\lambda(\pi) = -\lambda(-\pi)$ and $z(\pi) = z(-\pi)$.

The homotopy classes of Hamiltonians with $SR \circ TR$ symmetry are thus homotopy classes of curves in a punctured $\lambda - z$ plane whose end-points are constrained to be mirror-images in the z -axis.

The end-points can be assumed to be on the $+z$ -axis (since any point and its mirror image can be moved continuously to $+z$). The curve now is closed so it has a winding number. If one of the end-points is taken around the origin n times and brought back (while the other end-point is always at the mirror image), the winding number changes by $2n$. Thus, there are only two classes, characterized by even and odd winding number around the origin after the end-points are moved to the $+z$ -axis. The curves with even winding number can be contracted to constants $\pm Z$ and the curves with odd winding number can be contracted to $-Z$ (by moving the two end-points half-way around a circle in opposite directions) so all Hamiltonians are $\cong \pm Z^9$.

⁹To distinguish between these two cases without first moving the end-points together, count the number of times the interior of the curve crosses the $-z$ axis. The parity is a homotopy invariant, and is equivalent to the previous classification.

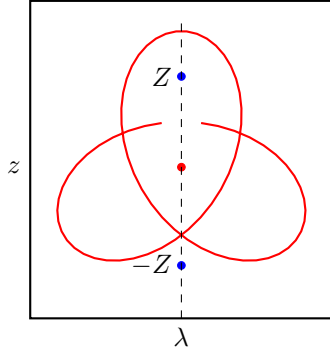


Figure 10: γ in the $\lambda-z$ plane. The curve can be retracted to Z by retracting the end point symmetrically relative to the z axis. The curve can not be retracted to $-Z$.

6 Changing unit cell permutes homotopy classes

The homotopy classes depend, in general, on the choice of unit cell [2, 25]. Different choices of unit cell are related by a gauge transformation, section 3.1,

$$H(k) \mapsto U_\ell^\dagger H(k) U_\ell, \quad U_\ell = \begin{pmatrix} 1 & 0 \\ 0 & e^{-ik\ell} \end{pmatrix}, \quad \ell \in \mathbb{Z} \quad (6.1)$$

Under such a transformation the equivalence classes transform as

$$Z \mapsto Z, \quad X \mapsto R_\ell, \quad R_n \mapsto R_{n+\ell}. \quad (6.2)$$

This does not mean that all the phases are equivalent, just that the labeling of the phase depends on how the unit cell is chosen. This may seem surprising, since in some cases the homotopy class is known to be related to the number of edge states. However, when a chain has an edge there is only one way to divide it up into unit cells so that no unit cell extends past the end.

7 Stable and Fragile Bloch bands

The problem considered here can be extended to larger matrices, to allow for the possibility of Hamiltonians with more orbitals. In that case the problem is to classify loops in the space of Hermitian matrices of a given dimension with a gap. That is, there is some value, the chemical potential, that the eigenvalues never cross. The chemical potential can be shifted to zero, so that no eigenvalue can ever be zero (i.e., the matrix is invertible). Fixing the number of occupied states to be m , the space of interest is thus set of $n \times n$ invertible matrices with m negative and $n - m$ positive eigenvalues. The phases of 2×2 Hamiltonians give a first hint about the phases that occur for larger matrices as the dimension can be increased by adding states with very high energies.

7.1 Fragile classes

A phase (with a given symmetry) is fragile [26] if its homotopy class changes when the dimension of the matrices of band projection $P(k)$ is increased:

$$P(k) \mapsto \begin{pmatrix} P(k) & 0 \\ 0 & 0 \end{pmatrix} \quad (7.1)$$

Consider an $n \times n$ real, periodic, projection $P(k)$ onto a single band:

$$P(k) = P^*(k) = P(k + 2\pi) = P^2(k), \quad \text{Tr } P(k) = 1 \quad (7.2)$$

Here reality plays the role of a symmetry constraint¹⁰. Since $P(k)$ is a real symmetric matrix it can be diagonalized by an orthogonal transformation and its non-trivial eigenvector

$$P(k) |k\rangle = |k\rangle \quad (7.3)$$

can be chosen to be real vectors of unit length in \mathbb{R}^n . The eigenvalue equation then determines $|k\rangle$ uniquely, up to a ± 1 phase ambiguity. Since $P(k)$ is continuous in k , we may choose $|k\rangle$ so that it is a continuous family for $k \in [-\pi, \pi]$. Then $|k\rangle$ traces a continuous curve on the unit sphere in \mathbb{R}^n . Since $P(-\pi) = P(\pi)$ and $|k\rangle$ has ± 1 phase freedom, the curve is either a closed loop or one with antipodal end-points:

$$|k = -\pi\rangle = \pm |k = \pi\rangle \quad (7.4)$$

The \pm alternative divides the space of curves $|k\rangle$ on the sphere into two classes: A symmetric class where $|k = \pi\rangle = |k = -\pi\rangle$ and an anti-symmetric class where $|k = \pi\rangle = -|k = -\pi\rangle$. This holds for any $n \geq 2$.

In the case $n = 2$ the curves can be classified further according to the winding number of $|k\rangle$ on the circle, which is a whole number (for the symmetric class) or a half-integer for the anti-symmetric class, see Fig. 7.1.

To relate this to the winding number of the curve γ representing the Hamiltonian, note that since H is real, γ is in the $x - z$ plane. This curve winds twice as fast as the eigenvector, so its winding number is an integer (as expected since the Hamiltonian must be periodic). It is odd for an anti-symmetric eigenvector and even for a symmetric one.

For $n \geq 3$ the vector $|k\rangle$ lies on \mathbb{S}^{n-1} which is simply connected, so all integer winding can be undone, reducing to a single class for the symmetric case and a single class for the anti-symmetric case.

Thus, we find that the periodic real projections $P(k)$ are labeled by invariants as follows:

$$\begin{aligned} \mathbb{Z}, & \quad n = 2 \\ \mathbb{Z}_2, & \quad n \geq 3 \end{aligned}$$

Hence all real Bloch bands with an even winding number of γ collapse to a single equivalence class, while those with an odd winding number collapse to a second equivalence class, once the dimension of the Hamiltonian is increased above 2.

¹⁰It is BR \circ TR upon a change of basis.

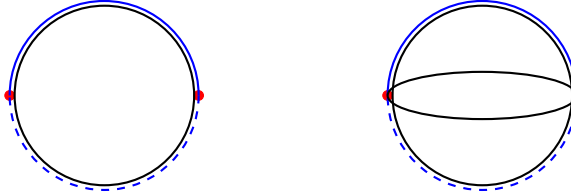


Figure 11: The blue solid semi-circle and the dashed semi-circle are homotopically distinct when the embedding space is the plane but are equivalent in three dimensions.

7.2 Stable Topological Classes

When the number of bands increases, the classification changes in two ways—fragile classes become equivalent to trivial classes as above and some new classes that could not exist with just one band appear. The classification turns out to have a more universal form, called “stable.”

As an example consider all the classes in the table that involve either SR or BR (there are three of each). The table shows that SR and BR behave differently for 2×2 matrices, however, as we shall see, their “stable” classes are the same.

One would expect this based on the relationship to Schrödinger Hamiltonians. A chain can be used as a model for a Schrödinger Hamiltonian with a periodic potential. For example space can be discretized into many sites. When the sites are closely spaced, the classification into phases should not depend on whether the inversion centers are on sites or between sites.

Consider insulators with just reflection symmetry (either bond or site reflection). The reflection transformation (either X or G_k for the 2×2 case) commutes with $H(k)$ for $k = 0, \pi$. So eigenstates of H are also eigenvectors of reflection; we can define an invariant $N_-(k)$ if $k = 0$ or π : Let $N_-(k)$ be the number of negative energy eigenstates of $H(k)$ with eigenvalues -1 for reflection. (The number of negative energy states with eigenvalues $+1$ is not a separate invariant since the total number of negative eigenvalues is fixed.) These can be shown to be the only homotopy invariants (see [27]). Finally, $N_-(0) - N_-(\pi)$ is especially interesting because when it is nonzero it implies that the band projection $P(k)$ cannot be deformed to a k -independent matrix. (Hence there is no insulator in the same phase whose wave function factors).

Table 1 has only 4 classes for BR and 2 for SR instead of infinitely many because $N_-(0), N_-(\pi)$ cannot be greater than 1 for 2×2 matrices! But these two or four phases otherwise fit into this classification system, as they differ in whether the occupied states at 0 and π are even or odd under inversion symmetry¹¹.

Now consider $BR \circ TR$ and $SR \circ TR$. According to table 1, the homotopy

¹¹The reason site and bond inversion are different is that the matrix $G(k)$ which describes site inversion is the identity at $k = 0$ so automatically $N_-(0) = 0$.

classes are labeled by \mathbb{Z} and \mathbb{Z}_2 respectively. For larger matrices, the labeling is by \mathbb{Z}_2 in both cases. The \mathbb{Z} invariant of $\text{BR} \circ \text{TR}$ is fragile for matrices of more than 2 dimensions. ($\text{BR} \circ \text{TR}$ symmetry implies $H(k) = XH^*(-k)X$, which can be transformed to $H(k) = H^*(-k)$ by changing the basis, so this reduces to the problem studied in the previous section.)

Finally, when there is both time reversal and inversion symmetry, the classes can be shown to be exactly the same as if inversion symmetry only is present—they can be labelled by a pair of natural numbers $N_-(0)$ and $N_-(\pi)$.

8 Concluding remarks

Our aim here was to give an elementary invitation to the field of topological insulators by studying the homotopic classification of 2×2 simple (=non-degenerate) periodic matrices in one dimension with various symmetries. Using simple intuitive facts about the homotopy of curves, we have shown how various symmetries are expressed in the homotopic classification of Bloch Hamiltonians. We have also presented an introduction to the notions of fragile and stable topological phases.

Acknowledgement

JA thanks Johannes Kellendonk, Oded Kenneth, Roy Meshulam, Daniel Podolsky, Immanuel Bloch and Raffaele Resta for useful discussions.

A Chiral symmetry

Chiral (or Sub-lattice) map is a unitary map that preserves k ,

$$H(k) \mapsto UH(k)U^\dagger, \quad U^2 = \mathbb{1} \quad (\text{A.1})$$

$H(k)$ has chiral symmetry¹² if it anti-commutes with U

$$H(k) = -UH(k)U^\dagger \quad (\text{A.2})$$

Since $U^2 = \mathbb{1}$ the eigenvalues of U are ± 1 . The case $U = \pm \mathbb{1}$ is trivial since it leads to $H(k) = 0$. In the case the two eigenvalues are distinct U is unitarily equivalent to a Pauli matrix. Choose a basis so $U = Z$. From

$$\{Z, H(k)\} = 0 \quad (\text{A.3})$$

we have¹³

- The curve γ lies in a punctured $x - y$ plane.

Chiral symmetry is the same as symmetry under the *composition* of particle hole and time reversal symmetry.

¹²This notion of chirality seems to have little to do with the common notion of chirality as the correlation between spin direction and the velocity.

¹³Had we chosen $U = Y$ chiral symmetry would mean that $H(k)$ is a real symmetric matrix.

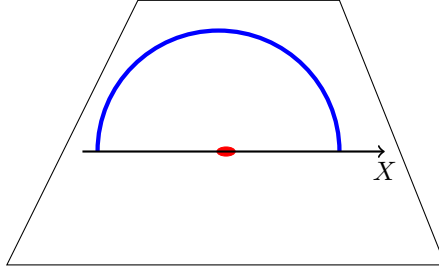


Figure 12: The half-loop associated with particle-hole symmetric Hamiltonians is anchored on the punctured x -axis. The rest of the loop is fixed by symmetry.

A.1 Homotopy classes for chiral symmetry

Chiral symmetry says that γ lies in a punctured plane which is not simply connected:

$$\pi_1(\mathbb{R}^2/\{0\}) = \mathbb{Z} \quad (\text{A.4})$$

The homotopy classes can be labeled by the the winding of γ (assumed to lie in the $x - y$ plane). $H(k)$ with winding n is homotopic to¹⁴

$$R_n = \begin{pmatrix} 0 & e^{-ink} \\ e^{ink} & 0 \end{pmatrix} \quad (\text{A.5})$$

$R_n \cong -R_n$ by rotation by π around the z - axis. (A rotation that respects the symmetry.) It follows that chiral Bloch Hamiltonians are homotopic to

$$\{H(k), k \in \mathbb{S}\} \cong \{R_n | n \in \mathbb{Z}\} \quad (\text{A.6})$$

A.1.1 Homotopy classes for particle hole and time reversal symmetry

Particle hole and chiral symmetry together also imply symmetry under their composition, chiral symmetry. Chiral symmetry restricts γ to the $x - y$ plane and time reversal forces the anchoring points to lie in the $x - z$ plane. It follows that the anchoring points at $0, \pi$ must lie on a punctured x -axis. γ and $-\gamma$ are homotopically distinct since a rotation about the z -axis changes the anchored points. This doubles the homotopy classes

$$R_n \mapsto \pm R_n. \quad (\text{A.7})$$

To summarize

$$\{H(k), k \in \mathbb{S}\} \cong \{\pm R_n | n \in \mathbb{Z}\} \quad (\text{A.8})$$

¹⁴Note that $\text{winding}(e^{ik}) = \text{winding}(-e^{ik})$

References

- [1] F. Duncan M. Haldane. Nobel lecture: Topological quantum matter. *Reviews of Modern Physics*, 89(4):040502, 2017.
- [2] Liang Fu, Charles L. Kane, and Eugene J. Mele. Topological insulators in three dimensions. *Physical Review Letters*, 98(10):106803, 2007.
- [3] Alexei Kitaev. Periodic table for topological insulators and superconductors. In *AIP Conference Proceedings*, volume 1134, pages 22–30. American Institute of Physics, 2009.
- [4] Zheng-Cheng Gu and Xiao-Gang Wen. Tensor-entanglement-filtering renormalization approach and symmetry-protected topological order. *Physical Review B*, 80(15):155131, 2009.
- [5] Alexander Altland and Martin R. Zirnbauer. Nonstandard symmetry classes in mesoscopic normal-superconducting hybrid structures. *Physical Review B*, 55(2):1142, 1997.
- [6] Ching-Kai Chiu, Jeffrey C.Y. Teo, Andreas P. Schnyder, and Shinsei Ryu. Classification of topological quantum matter with symmetries. *Reviews of Modern Physics*, 88(3):035005, 2016.
- [7] Andreas P. Schnyder, Shinsei Ryu, Akira Furusaki, and Andreas W.W. Ludwig. Classification of topological insulators and superconductors in three spatial dimensions. *Physical Review B*, 78(19):195125, 2008.
- [8] Erez Berg, Michael Levin, and Ehud Altman. Quantized pumping and topology of the phase diagram for a system of interacting bosons. *Physical Review Letters*, 106(11):110405, 2011.
- [9] Alexei Kitaev. Anyons in an exactly solved model and beyond. *Annals of Physics*, 321(1):2–111, 2006.
- [10] Xie Chen, Zheng-Cheng Gu, and Xiao-Gang Wen. Local unitary transformation, long-range quantum entanglement, wave function renormalization, and topological order. *Physical Review B*, 82(15):155138, 2010.
- [11] Michael Levin and Xiao-Gang Wen. Detecting topological order in a ground state wave function. *Physical Review Letters*, 96(11):110405, 2006.
- [12] Hal Tasaki. *Physics and Mathematics of Quantum Many-Body Systems*. Springer International Publishing, 2020.
- [13] Yoshiko Ogata. A Z_2 -index of symmetry protected topological phases with time reversal symmetry for quantum spin chains. *Communications in Mathematical Physics*, 374(2):705–734, 2020.
- [14] Lukasz Fidkowski and Alexei Kitaev. Topological phases of Fermions in one dimension. *Physical Review B*, 83(7):075103, 2011.

- [15] Frank Pollmann, Ari M. Turner, Erez Berg, and Masaki Oshikawa. Entanglement spectrum of a topological phase in one dimension. *Physical Review B*, 81(6):064439, 2010.
- [16] Sven Bachmann, Spyridon Michalakis, Bruno Nachtergael, and Robert Sims. Automorphic equivalence within gapped phases of quantum lattice systems. *Communications in Mathematical Physics*, 309(3):835–871, 2012.
- [17] Sven Bachmann, Alex Bols, Wojciech De Roeck, and Martin Fraas. A many-body index for quantum charge transport. *Communications in Mathematical Physics*, 375(2):1249–1272, 2019.
- [18] Bertrand I. Halperin. Quantized hall conductance, current-carrying edge states, and the existence of extended states in a two-dimensional disordered potential. *Physical Review B*, 25(4):2185, 1982.
- [19] Gian Michele Graf and Marcello Porta. Bulk-edge correspondence for two-dimensional topological insulators. *Communications in Mathematical Physics*, 324(3):851–895, 2013.
- [20] Jason Alicea, Yuval Oreg, Gil Refael, Felix von Oppen, and Matthew P. A. Fisher. Non-abelian statistics and topological quantum information processing in 1d wire networks. *Nature Physics*, 7(5):412–417, 2011.
- [21] Chetan Nayak, Steven H. Simon, Ady Stern, Michael Freedman, and Sankar Das Sarma. Non-abelian anyons and topological quantum computation. *Reviews of Modern Physics*, 80(3):1083, 2008.
- [22] Julia Kempe, Alexei Kitaev, and Oded Regev. The complexity of the local Hamiltonian problem. *Siam Journal on Computing*, 35(5):1070–1097, 2006.
- [23] Emil Prodan and Hermann Schulz-Baldes. *Bulk and boundary invariants for complex topological insulators: From K-theory to physics*. Springer, 2016.
- [24] Jacob Shapiro. *Topology and Localization: Mathematical Aspects of Electrons in Strongly-Disordered Media*. PhD thesis, ETH Zurich, 2018.
- [25] Shinsei Ryu and Yasuhiro Hatsugai. Entanglement entropy and the berry phase in the solid state. *Physical Review B*, 73(24):245115, 2006.
- [26] Hoi Chun Po, Haruki Watanabe, and Ashvin Vishwanath. Fragile topology and Wannier obstructions. *Physical Review Letters*, 121(12):126402, Sep 2018.
- [27] Ari M. Turner, Yi Zhang, Roger S. K. Mong, and Ashvin Vishwanath. Quantized response and topology of magnetic insulators with inversion symmetry. *Physical Review B*, 85(16):165120, 2012.